Electronic Preprint for Journal of Information Processing Vol.25

Regular Paper

The Complexity of Generalized Pipe Link Puzzles

Akihiro Uejima[1,a)] Hiroaki Suzuki[1] Atsuki Okada[1]

Received: November 7, 2016, Accepted: May 16, 2017

Abstract: Pipe Link, which is a pencil-and-paper puzzle introduced by Japanese puzzle publisher Nikoli, is played on a rectangular grid of squares. We studied the computational complexity of Pipe Link, and this paper shows that the problem to decide if a given instance of Pipe Link has a solution is **NP**-complete by a reduction from the Hamiltonian circuit problem for a given planar graph with a degree of at most 3. Our reduction is carefully designed so that we can also prove **ASP**-completeness of the another-solution-problem.

Keywords: computational complexity, NP-complete, ASP-complete, pencil-and-paper puzzle, Pipe Link

1. Introduction and Definitions

Pencil-and-paper puzzles, which consist of figures or words on paper, are solved by a person drawing on the figure with a pencil. Pipe Link is one of many pencil-and-paper puzzles made popular by Nikoli [9], which is a famous Japanese publisher of such puzzles. The Pipe Link puzzle is played on a rectangular grid of squares with pieces of a path, and the objective of the puzzle is to draw a single closed loop containing all the given path pieces on the grid. In this paper, we examine the complexity of the Pipe Link puzzle.

For many people, the fun of completing games and puzzles comes from the difficulty in finding a solution. From this point of view, the computational complexity of many games and puzzles has been widely studied, and it is known that many commonly played puzzles are **NP**-complete. For example, in 2009, Hearn and Demaine [4] surveyed the computational complexities of combinatorial games and puzzles. Hashiwokakero [1], Number Link [8], Kurodoko [7], Shikaku and Ripple Effect [11], Yajilin and Country Road [5], Yosenabe [6], Shakashaka [3], Fillmat [12], etc., are pencil-and-paper puzzles published by Nikoli. Recent studies have shown that all of these are **NP**-complete and/or **ASP**-complete. However, the complexity of Nikoli's pencil-and-paper puzzle named Pipe Link has not been previously studied. Thus, in this paper, we study the computational complexity of deciding whether Pipe Link has a solution.

An instance of Pipe Link and its solution are shown in **Fig. 1**. Pipe Link is played on a rectangular grid B of size $m \times n$. Lines, such as the ones shown in **Fig. 2**, are drawn in some of the squares as input. We call these pre-given lines *clue pieces* for solving the puzzle. The player's task is to construct a single closed loop containing all the clue pieces in B by drawing any of the candidate lines shown in Fig. 2 in each blank square so that the following rules (1) to (4) mentioned below are satisfied. The seven types of candidates are shown in Fig. 2 and are called I_1, I_2, L_1, L_2, L_3, L_4, and X *pipes*. Throughout this paper, blue colored pipes represent clue pieces and red colored pipes represent pipes placed by the player in B (and/or gadgets). The rules of Pipe Link are as follows.

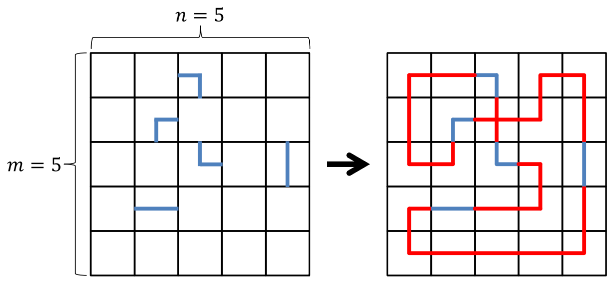

Fig. 1 Instance of Pipe Link and its solution.

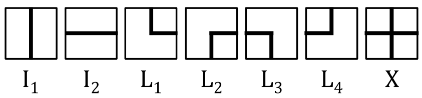

Fig. 2 Types of lines drawn in squares.

(1) A pipe must be placed in every blank square, which is a square without clue pieces.
(2) No lines can be added to the squares with clue pieces.
(3) X pipes represent the three-dimensional intersection of two straight lines.
(4) The segments of the line loop run horizontally or vertically between the center points of orthogonally adjacent squares.

We note that all squares have pipes in the solution shown in Fig. 1, and all of the blue and red lines in Fig. 1 form a single closed loop. The loop includes a crossover of two straight lines. Of course, all solutions of instances do not need to include an X pipe. In this paper, we mainly consider the decision problem of Pipe Link, defined as follows.

Pipe Link Decision Problem

Instance: A rectangular grid B of size $m \times n$, with some squares having clue pieces.

[1] Osaka Electro-Communication University, Neyagawa, Osaka 572–8530, Japan
[a)] uejima@isc.osakac.ac.jp

Question: Is there an arrangement of pipes on the blank squares in B satisfying the above constraints (1) to (4)?

We analyze the computational complexity of the decision problem above and the another-solution-problem (**ASP**) of Pipe Link, and we show the following theorems in this paper (see Ref. [13] for definitions of **ASP** and **ASP**-completeness).

Theorem 1. *Pipe Link Decision Problem is **NP**-complete.*

Theorem 2. *The another-solution-problem of Pipe Link is **ASP**-complete.*

Theorem 1 is a direct corollary from both Theorem 2 and the discussion in Ref. [13] (see Theorem 3.4 in Ref. [13]).

2. Proof of Theorems 1 and 2

We are now ready to state and prove our claim of **NP**-completeness and **ASP**-completeness. Because it can be verified whether a solution candidate is correct in polynomial time, it is obvious that the problem to decide whether an instance of Pipe Link has a solution is in **NP**.

To prove **NP**-hardness, we construct a reduction from the Hamiltonian circuit problem (HCP) for a given planar graph with a degree of at most 3 (i.e., restricted HCP). In restricted HCP, the problem is deciding whether a given graph $G = (V, E)$ has a circuit that visits every vertex $v \in V$ exactly once. In Ref. [13], the **ASP** variant of the Hamiltonian circuit problem has already been shown to be **ASP**-complete (see also Ref. [10] for more details of the proof). Moreover, that research also showed that Slither Link, which is one of Nikoli's pencil puzzles, is ASP-complete by constructing an ASP reduction from the restricted HCP (see Ref. [13] for the definition of the term "**ASP** reduction").

We prove Theorems 1 and 2 by constructing an ASP reduction from the restricted HCP with a technique similar to that in Ref. [13]. Namely, our reduction is carefully designed so that each solution of Pipe Link has a one-to-one correspondence with a solution of the original instance of HCP. Therefore, the reduction also implies the result for the ASP of Pipe Link. The **ASP** version of Pipe Link is defined as follows: Given an instance P consisting of a grid B with clue pieces of Pipe Link and a solution s, find a solution s' of P other than s. We use the following known fact in Ref. [2] for our reduction.

Lemma 1. *Reference [2] Any planar graph $G = (V, E)$ with a degree of at most 3 can be embedded in an $O(|V| \times |V|)$ grid in polynomial time in $|V|$.*

By using Lemma 1, we can transform a given graph G of the restricted HCP into a graph G' on the grid, as shown in **Fig. 3**. We note that G' has lattice points that do not correspond to the vertices of graph G, and such points need not be visited in Hamiltonian circuits of G'. The degree of such lattice points is two. Throughout this paper, the white colored circles illustrated in Fig. 3 represent points that do not correspond to the vertices of graph G, and we call such points in G' *white vertices*. Similarly, the black colored circles represent lattice points that do correspond to the vertices of G and thus must be visited in Hamiltonian circuits of G'. We call such points in G' *black vertices*.

We assume that an input graph $G = (V, E)$ is embedded as a graph $G' = (V', E')$ with $p = O(|V|)$ vertices in the vertical direction and $q = O(|V|)$ vertices in the horizontal direction on the grid. Thus, $|V'| \leq p \times q$.

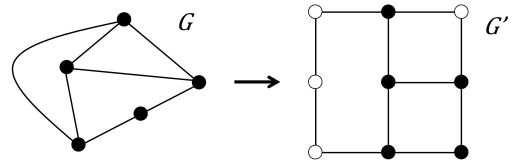

Fig. 3 Conversion to a graph on the grid.

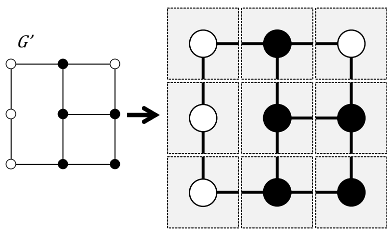

Fig. 4 Brief image of our reduction.

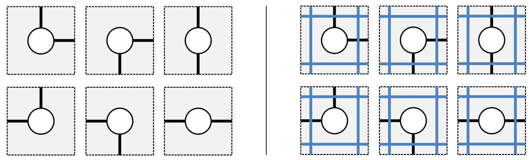

(a) without auxiliary lines (b) with auxiliary blue-lines

Fig. 5 Gadget for a white vertex in G'.

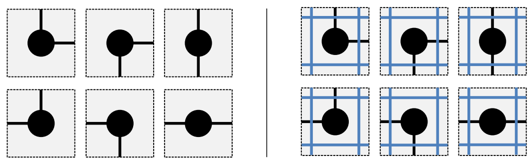

(a) without auxiliary lines (b) with auxiliary blue-lines

Fig. 6 Gadget for a black vertex with degree 2 in G'.

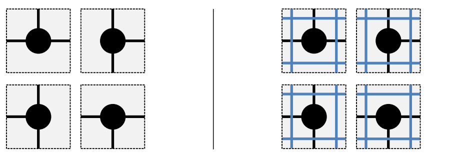

(a) without auxiliary lines (b) with auxiliary blue-lines

Fig. 7 Gadget for a black vertex with degree 3 in G'.

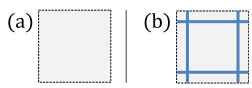

Fig. 8 Gadget for unchosen points in G'.

The brief image of our reduction is as follows. We construct gadgets corresponding to the white and black vertices of G', and we place the gadgets according to the layout of graph G' embedded on the grid, as shown in **Fig. 4**. By considering the number of degrees and the embedded way of edges, all necessary gadgets for the white and black vertices can be shown on the left sides of **Fig. 5**, **Fig. 6**, **Fig. 7**, and **Fig. 8** (note that some points could be neither white vertices nor black vertices). On the other hand, the figures shown on the right sides of Fig. 5, Fig. 6, Fig. 7, and Fig. 8 are brief images of gadgets with blue auxiliary lines for implementing the functions of the vertex gadgets. We will construct four partial paths consisting of clue pieces in order to surround

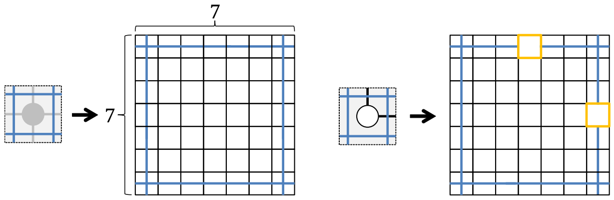

Fig. 9 Outline of vertex gadgets and gateways.

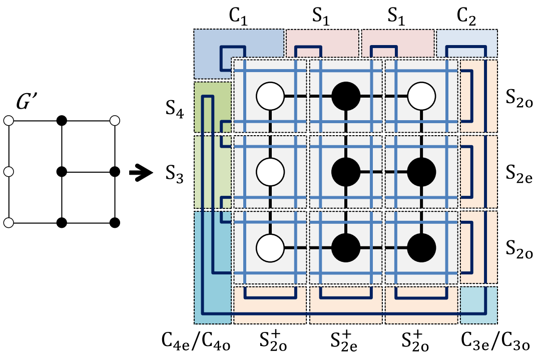

Fig. 10 Outline of our reduction.

the periphery of the gadgets.

In our construction of the vertex gadgets, we consider 7×7 squares to be the basic unit, as shown in **Fig. 9**. The vertex gadgets have gateways on the middle of the left, right, top, and bottom sides of the 7×7 squares. The gateways depend on the existence or nonexistence of edges incident to the vertex, as shown in Fig. 9. For example, the upper left gadget in the figure of Fig. 5 (a) has clue pieces in the periphery of the gadget as auxiliary lines, except for the middle squares of the right and top sides, as illustrated in the right figure of Fig. 9.

In the following section, we construct gadgets corresponding to the white and black vertices of G'. We also construct some gadgets that connect auxiliary lines in the vertex gadgets as a single loop; these gadgets are called *wall gadgets*.

2.1 Outline of Reduction and Wall Gadgets

An outline of our reduction is shown in **Fig. 10**. We put wall gadgets around the vertex gadgets introduced in the previous section, as illustrated in Fig. 10. Namely, we put gadgets S_1, C_2, S_{2o}, S_{2e}, C_{3e}/C_{3o}, S^+_{2o}, S^+_{2e}, C_{4e}/C_{4o}, S_3, and S_4 in the clockwise direction with respect to wall gadget C_1, which is set in the upper left of Fig. 10. We call gadgets C_* and S_* *corner-wall* gadgets and *side-wall* gadgets, respectively.

We next describe in more detail the arrangement of the wall gadgets. As stated above, G is embedded as a graph G' with p vertices in the vertical direction and q vertices in horizontal direction on the grid. In **Fig. 11**, $q-1$ gadgets S_1 are placed on the top side, and gadgets S_{2o} and S_{2e} are placed alternately on the right side. We note that gadget C_{3e} is placed on the lower right if p is odd; otherwise, C_{3o} is placed on the lower right. Similarly, S^+_{2o} and S^+_{2e} are placed alternately from right to left on the bottom side. Gadget C_{4e} is placed on the lower left if q is odd; otherwise, C_{4o} is placed on the lower left. After that, $p-2$ gadgets S_3 are placed from the bottom up on the left side, and the last gadget S_4 is placed on the left side, as illustrated in Fig. 11.

Each wall gadget is constructed to have partial paths consisting

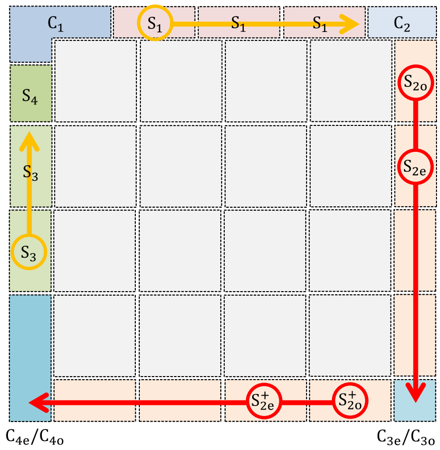

Fig. 11 Layout of wall gadgets.

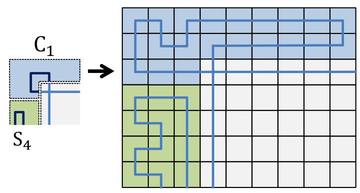

Fig. 12 Corner-wall gadget C_1.

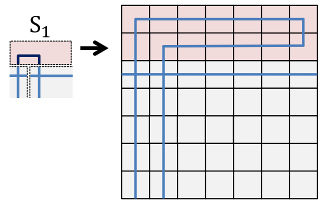

Fig. 13 Top side-wall gadget S_1.

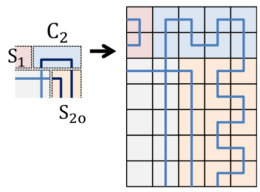

Fig. 14 Corner-wall gadget C_2.

of clue pieces, as shown by the dark blue lines in Fig. 10. Thus, all of the auxiliary lines in the vertex gadgets and the partial paths in the wall gadgets construct a single closed loop (see the blue and dark blue colored lines in Fig. 10).

The details of the corner-wall gadgets and the side-wall gadgets are shown in the figures of **Fig. 12**, **Fig. 13**, **Fig. 14**, **Fig. 15**, **Fig. 16**, **Fig. 17**, **Fig. 18**. We note that gadgets S^+_{2o} and S^+_{2e} are obtained by 90-degree rotation of S_{2o} and S_{2e} in the clockwise direction, respectively. Moreover, all squares in the wall gadgets are clue pieces, and thus all corner-wall gadgets and side-wall gadgets satisfy rule (1).

2.2 White Vertex Gadget

In this section, we show the gadgets for the white vertices of G'. These are called *white vertex gadgets*. Though the six types of gadgets were introduced as necessary shapes in Fig. 5, due to rotational symmetry, it is to sufficient to construct two types of white vertex gadgets W_1 and W_2, as illustrated in **Fig. 19** and

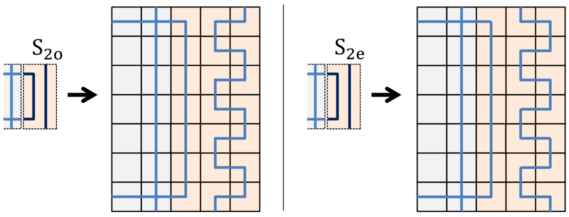

(a) Odd-numbered case (b) Even-numbered case

Fig. 15 Right side-wall gadgets S_{2o} and S_{2e}.

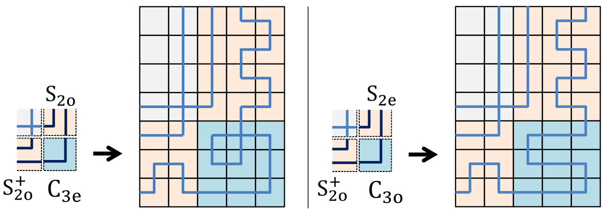

(a) If the above is S_{2o} (b) If the above is S_{2e}

Fig. 16 Corner-wall gadgets C_{3e} and C_{3o}.

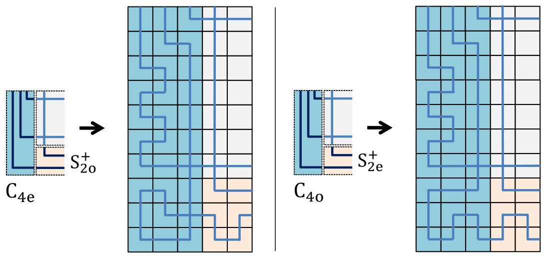

(a) If the right is S^{+}_{2o} (b) If the right is S^{+}_{2e}

Fig. 17 Corner-wall gadgets C_{4e} and C_{4o}.

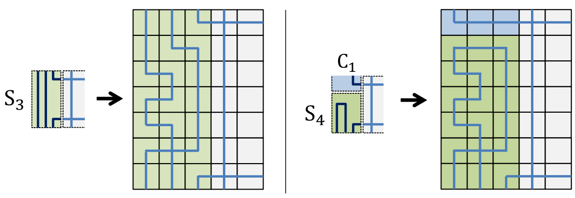

(a) If the above is not C_1 (a) If the above is C_1

Fig. 18 Left side-wall gadgets S_3 and S_4.

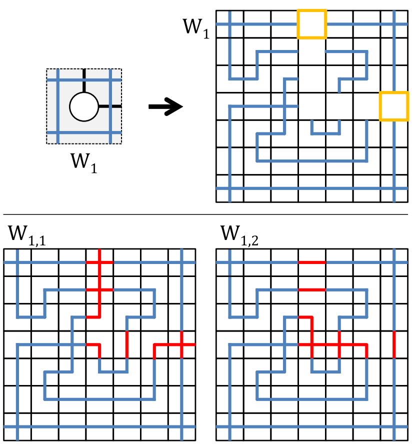

Fig. 19 White vertex gadget and its local solutions.

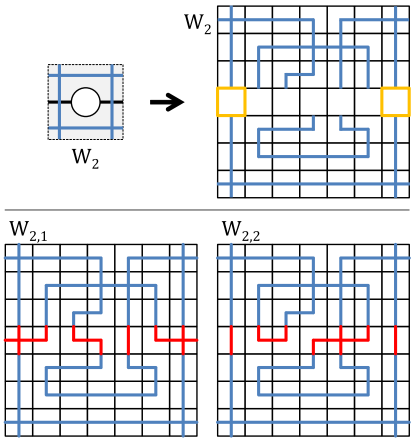

Fig. 20 Another white vertex gadget and its local solutions.

Fig. 20.

The gadget W_1 in Fig. 19 has 7 blank squares, including two yellow colored ones on the middle of the right and top sides. We next consider the way to draw lines in the blank square at the middle of the top side. According to the clue pieces in the right and left squares, we can put either the X or the I_2 pipe on this blank square. If we place the X pipe, the way to draw lines in the rest of the blank squares is fixed as $W_{1,1}$ in Fig. 19; otherwise, $W_{1,2}$ is fixed in Fig. 19. $W_{1,1}$ consists of (i) the path associated with the auxiliary lines, and (ii) the path connecting the two yellow colored squares. On the other hand, $W_{1,2}$ consists of only the path associated with the auxiliary lines. These are expressed according to whether the white vertex in the Hamiltonian circuits of G' is visited.

W_2 in Fig. 20 is also constructed similarly to W_1. The gadget W_2 has 7 blank squares in a row and includes two yellow colored squares on the middle of the right and left sides. In this case also, the way to draw the lines is determined in two ways. We focus on the square at the middle of the left side. We can put either the X or the I_1 pipe on this blank square, because the adjacent squares above and below have clue pieces I_1. If placing the X pipe, the way to draw lines on the rest of the blank squares is fixed as $W_{2,1}$ in Fig. 20; otherwise, $W_{2,2}$ is fixed in Fig. 20. We note that these drawings in W_2 are expressed regardless of whether the white vertex in the Hamiltonian circuits of G' is visited.

We obtain the remaining types of gadgets shown in Fig. 5 by rotating W_1 and W_2. For example, the type in the upper middle of Fig. 5 (a) is obtained by 90-degree rotation of W_1 in the clockwise direction.

2.3 Black Vertex Gadget

In this section, we show the gadgets for the black vertices of G'. These are called *black vertex gadgets*. We introduced the ten types of gadgets as necessary shapes in Fig. 6 and Fig. 7.

If we pay attention to the fact that the black vertices in G' must be visited in Hamiltonian circuits, we can divert the local solutions $W_{1,1}$ and $W_{2,1}$ of the white vertex gadgets to the gadgets for a black vertex with degree 2 by changing all red lines of $W_{1,1}$ and $W_{2,1}$ to blue lines (i.e., clue pieces). Moreover, for the gadgets of a black vertex with degree 3 (see Fig. 7), due to the rotational symmetry, it is to sufficient to construct one type of black vertex gadget, B_1, as illustrated in **Fig. 21**.

The gadget B_1 in Fig. 21 has 10 blank squares, including three yellow ones at the middle of the left, right, and top sides, and a red one at the center. We consider the way to draw lines in the blank

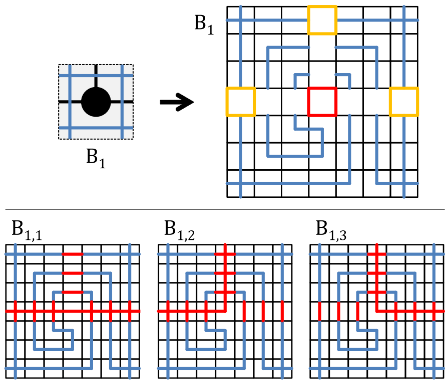

Fig. 21 A black vertex gadget and its local solutions.

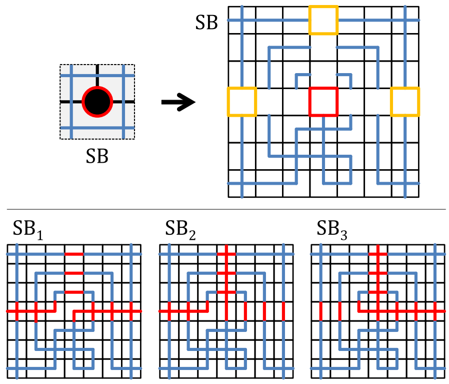

Fig. 23 SB gadget and its local solutions.

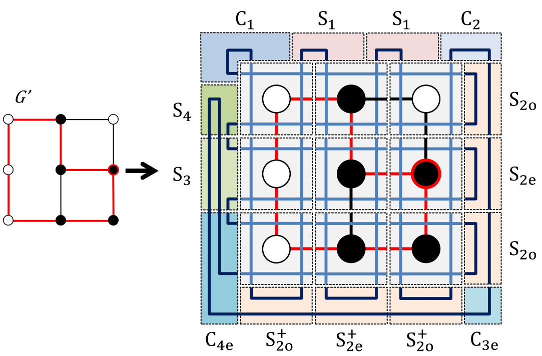

Fig. 22 Proof of correctness of the reduction.

square colored red at its center. Because the square below has the clue piece L_3, we can put the I_1, L_4, or L_1 pipe in this blank square. If we place the I_1 pipe, the way to draw lines in the rest of the blank squares is fixed as $B_{1,1}$ in Fig. 21. Moreover, if we place the L_4 pipe, the way to draw lines for the gadget is fixed as $B_{1,2}$; otherwise, $W_{1,3}$ is fixed, as in Fig. 21. $B_{1,1}$, $B_{1,2}$, and $B_{1,3}$ in Fig. 21 consist of (i) the path associated with the auxiliary lines, and (ii) the path connecting any two squares of the three squares colored yellow, as in the case of $W_{1,1}$ of gadget W_1 (also $W_{2,1}$ of gadget W_2). These three types (i.e., I_1, L_4, and L_1 pipes) represent the way to pass the black vertex of G' in the Hamiltonian circuit.

In addition, we explain the gadgets shown in Fig. 8. The lattice points are not expressed as white vertices or black vertices. Therefore, we can use the local solutions $W_{1,2}$ and $W_{2,2}$ of the white vertex gadgets by changing all red lines of $W_{1,2}$ and $W_{2,2}$ to blue lines (i.e., clue pieces).

2.4 Black Vertex Gadget for Connecting Two Closed Loops

In this section, we show the black vertex gadget with a special feature. As stated in the previous sections, gadgets that act like a white or black vertex could be constructed. However, in the current situation, the rectangular grid B has two closed loops, as illustrated in **Fig. 22**: (i) the first loop, which is colored blue and dark blue, comprises auxiliary lines connecting the vertex gadgets and wall gadgets, and (ii) another loop, which is colored red, corresponds to the Hamiltonian circuits of G'. This situation is contrary to the rule of a single closed loop.

To overcome this deficiency, we show a special black vertex gadget for connecting two loops. It is called the *SB gadget*. We show the SB gadget corresponding to the B_1 gadget in **Fig. 23**. As in the case of B_1, other types of SB gadgets can be obtained by the rotation operation. The gadget SB in Fig. 23 has 10 blank squares, including three yellow ones at the middle of the left, right, and top sides, and a red one at the center. Because the square below the square colored red has the clue piece X, we can put the L_2, I_1, or X pipe in this blank square. The results are shown as SB_1, SB_2, and SB_3 in Fig. 23, respectively. We note that SB_1, SB_2, and SB_3 in Fig. 23 connect (i) the path associated with the auxiliary lines and (ii) the path expressing a way to visit the black vertex of G' in the Hamiltonian circuits.

By replacing any one gadget for a black vertex with degree 3 with the SB gadget rotated as needed, our reduction is completed. For example, in the reduction shown in Fig. 22, we replaced the middle right gadget B_1 by the gadget obtained by 270-degree rotation of SB in the clockwise direction, as shown in Fig. 23.

3. Proof of Correctness of the Reduction

All the necessary gadgets we listed were constructed in the previous section. In the way described in the previous section, we obtain the instance of Pipe Link corresponding to G' (that is, G). This reduction can be done in the polynomial time of the input size of the restricted HCP. The solution of Pipe Link corresponding to the Hamiltonian circuit of G is unique. Thus, we constructed a polynomial time ASP reduction from the restricted HCP for the Pipe Link puzzle. Therefore, the Pipe Link Decision Problem is **NP**-complete, and the **ASP** version of Pipe Link is **ASP**-complete.

4. Conclusions

In this paper, we studied the computational complexity of Pipe Link and proved that Pipe Link is **NP**-complete and **ASP**-complete by reducing the Hamiltonian circuit problem for a given planar graph with a degree of at most 3.

Acknowledgments This research was supported in part by the Institute of Informatics, Osaka Electro-Communication University.

References

[1] Andersson, D.: Hashiwokakero is NP-complete, *Inf. Process. Lett.*, Vol.109, No.19, pp.1145–1146 (2009).

[2] Battista, G.D., Eades, P., Tamassia, R. and Tollis, I.G.: Algorithm for Drawing Graphs: An Annotated Bibliography, *Computational Geometry*, Vol.4, No.5, pp.235–284 (1994).

[3] Demiane, E.D., Okamoto, Y., Uehara, R. and Uno, Y.: Computational Complexity and an Integer Programming Model of Shakashaka, *IEICE Trans. Fundamentals of Electronics, Communications and Computer Science*, Vol.E97-A, No.6, pp.1213–1219 (2014).

[4] Hearn, R.A. and Demaine, E.D.: *Game, Puzzles, & Computation*, A.K. Peters Ltd., MA, USA (2009).

[5] Ishibashi, A., Sato, Y. and Iwata, S.: NP-completeness of Two Pencil Puzzles: Yajilin and Country Road, *Utilitas Mathematica*, Vol.88, pp.237–246 (2012).

[6] Iwamoto, C.: Yosenabe is NP-complete, *J. Inf. Process.*, Vol.22, No.1, pp.40–43 (2014).

[7] Kölker, J.: Kurodoko is NP-complete, *J. Inf. Process.*, Vol.20, No.3, pp.694–706 (2012).

[8] Kotsuma, K. and Takenaga, Y.: NP-completeness and Enumeration of Number Link Puzzle, *IEICE Technical Report*, Vol.109, No.465, pp.1–7 (2010) (in Japanese).

[9] Nikoli: Rules of Pipe link (online, in Japanese), available from ⟨http://www.nikoli.co.jp/ja/puzzles/pipe_link/⟩ (accessed 2016-11-03).

[10] Seta, T.: The Complexities of Puzzles, CROSS SUM, and Their Another Solution Problems (ASP), Senior Thesis, University of Tokyo (2002).

[11] Takenaga, Y., Aoyagi, S., Iwata, S. and Kasai, T.: Shikaku and Ripple Effect are NP-Complete, *Congressus Numerantium*, Vol.216, pp.119–127 (2013).

[12] Uejima, A. and Suzuki, H.: Fillmat is NP-Complete and ASP-Complete, *J. Inf. Process.*, Vol.23, No.3, pp.310–316 (2015).

[13] Yato, T. and Seta, T.: Complexity and Completeness of Finding Another Solution and its Application to Puzzles, *IEICE Trans. Fundamentals of Electronics, Communications and Computer Sciences*, Vol.E86-A, No.5, pp.1052–1060 (2003).

Akihiro Uejima was born in 1975. He received his B.E. and M.E. degrees from the Information Systems Engineering, Department of Information and Computer Sciences, Toyohashi University of Technology in 1998 and 2000, respectively, and a Dr. of Informatics degree from the Department of Communications and Computer Engineering, Graduate School of Informatics at Kyoto University in 2005. He was a lecturer during 2005–2013, and has been an associate professor since 2013 in the Department of Engineering Informatics, Osaka Electro-Communication University. His research interest is in graph theory, computational complexity. He is a member of IEICE, IPSJ the Operations Research Society of Japan, the Language and Automaton Symposium.

Hiroaki Suzuki was born in 1991. He received a B.Sc. from the Department of Engineering Informatics, Faculty of Information and Communication Engineering, Osaka Electro-Communication University in 2014.

Atsuki Okada was born in 1994. He received a B.Sc. from the Department of Engineering Informatics, Faculty of Information and Communication Engineering, Osaka Electro-Communication University in 2016.